EXPERIMENTAL STUDY

Short-term autophagy inhibition by autophinib or SAR405 does not alter the effect of cisplatin on ATP production in prostate cancer cells

Monika KRATOCHVILOVA[1,2*], Petr STEPKA[2*], Martina RAUDENSKA[1,2,3], Jan BALVAN[1,2], Lukas RICHTERA[3], Natalia CERNEI[3], Dagmar STERBOVA SKOPALOVA[3], Ondrej ZITKA[3], Petr FILIPENSKY[4], Petr BABULA[2], Michal MASARIK[1,2,5]

Department of Physiology and Pathological Physiology, Faculty of Medicine, Masaryk University, Brno, Czech Republic. **masarik@med.muni.cz**

ABSTRACT

OBJECTIVES: Cisplatin is a widely used anticancer drug for the treatment of many solid cancers. DNA damage is thought to be the key mechanism of cisplatin's anticancer activity. However, cisplatin may also affect cellular metabolism. The aim of this study was to determine the effect of cisplatin on the types of ATP production (OXPHOS versus glycolysis) and their rate in prostate cancer cells and to determine the potentially protective effect of autophagy and amino acids during cisplatin treatment. We also wanted to investigate the potential synergy between the metabolic effects of cisplatin on ATP production and the inhibition of autophagy.
METHODS: We used two models of autophagy inhibition, a natural model of dysfunctional autophagy-DU145 cells and 24-hour inhibition of autophagy by autophinib or SAR405. The effect of cisplatin and autophagy inhibition was observed on prostate cancer cell lines 22Rv1, PC-3, and DU145. To assess the type (OXPHOS versus glycolysis) and rate of ATP production, the Seahorse XF Real-Time ATP Rate Assay was performed by measuring the extracellular acidification rates (ECAR) as a proxy for glycolytic readouts and the oxygen consumption rates (OCR) as a proxy for oxidative phosphorylation readouts. We also performed quantitative phase imaging and colony-forming assay to assess the metastatic potential of cancer cells. Finally, amino acid profiles were examined using ion-exchange liquid chromatography.
RESULTS: After cisplatin treatment, ATP production by OXPHOS was significantly decreased in 22Rv1 and PC-3 cells. On the other hand, ATP production by glycolysis was not significantly affected in 22Rv1 cells. DU145 cells with dysfunctional autophagy were the most sensitive to cisplatin treatment and showed the lowest ATP production. However, short-term autophagy inhibition (24h) by autophinib or SAR405 in 22Rv1 and PC-3 cells did not alter the effect of cisplatin on ATP production. Levels of some amino acids (arginine, methionine) significantly affected the fitness of cancer cells.
CONCLUSION: Persistent defects of autophagy can affect the metabolic sensitivity of cancer cells due to interference with arginine metabolism. Amino acids contained in the culture medium had an impact on the overall effect of cisplatin *(Fig. 3, Ref. 38)*. Text in PDF *www.elis.sk*
KEY WORDS: cisplatin, autophagy inhibition, amino acids, prostate cancer.

[1]Department of Pathological Physiology, Faculty of Medicine, Masaryk University, Brno, Czech Republic, [2]Department of Physiology, Faculty of Medicine, Masaryk University, Brno, Czech Republic, [3]Department of Chemistry and Biochemistry, Mendel University in Brno, Brno, Czech Republic, [4]Department of Urology, St. Anne's Faculty Hospital, Brno, Czech Republic, and [5]BIOCEV, First Faculty of Medicine, Charles University, Vestec, Czech Republic

Address for correspondence: Michal MASARIK, Prof, Department of Physiology and Pathological Physiology, Faculty of Medicine, Masaryk University, Kamenice 5, CZ-625 00 Brno, Czech Republic
Phone: +420.5.49493631, Fax: +420.5.49494340

*Monika Kratochvilova and Petr Stepka contributed equally to this work.

Introduction

Cis-diamminedichloroplatinum (II) (NSC 119875), more often referred to as cisplatin, is a widely utilized anticancer drug used against testicular cancer, malignancies of ovaries, and head and neck cancer (1, 2). However, the potential of cisplatin for treating primary prostate cancer is restricted due to its limited efficacy and toxic side effects. Nevertheless, cisplatin was shown to have some beneficial effects in advanced prostate cancer (3, 4). This effect of cisplatin in advanced prostate cancer is probably not caused by cell cycle arrest as the PC-3 cell line (derived from an androgen-independent and unresponsive metastatic site) does not show significant cell cycle arrest after cisplatin treatment (5).

It is widely recognised that the main mechanism of cisplatin's anti-cancer efficacy is based on its ability to impair DNA. However, cisplatin may also affect the metabolism and migration ability of

cancer cells (6, 7). Inside the cell, cisplatin loses chloride moieties and gains a positive charge, therefore it tends to accumulate in the negatively charged mitochondria, where cisplatin reacts with nucleophilic sites and forms DNA crosslinks (8). Cisplatin also induces mitochondrial ROS (mtROS) which is detrimental to the health of the cell. It was found that cisplatin-sensitive cells contain higher levels of mtROS than cells resistant to cisplatin. Mitochondrial ROS also correlates with the reduction of mitochondrial biogenesis (9). Depletion of PTEN in cancer cells can further impair mitochondrial structure and respiratory chain function (10). Consequently, cisplatin can impair mitochondrial respiration and oxidative phosphorylation (OXPHOS) predominantly in PTEN-depleted cells (8, 11). Cisplatin also downregulates the expression of many glycolysis-related proteins, including hexokinases, phosphofructokinases, pyruvate kinases, lactate dehydrogenase B, or glucose transporters 1 and 4 (GLUT-1/ *SLC2A1* and GLUT-4/*SLC2A4*) and exerts an inhibiting effect on glycolysis (7). Recent evidence in humans and mice supports the notion that mitochondrial metabolism is necessary for tumor growth. Tumor growth requires a functional electron transport chain for oxidation of ubiquinol, which is necessary to maintain oxidative TCA cycle function and activity of dihydroorotate dehydrogenase (DHODH) (12). DHODH donates electrons to mitochondrial ubiquinone during the conversion of dihydroorotate to orotate, which is a key step in *de novo* pyrimidine synthesis (13).

Furthermore, deregulation of the amino acid pool can affect tumor cell survival under anticancer treatment (14). As autophagy is often required for the maintenance of amino acid levels, we tested the effect of autophagy inhibition on the metabolic impacts of cisplatin. The correlation between levels of amino acids and the ability of cells to produce ATP was also assessed. We used two models of autophagy inhibition, a natural model of dysfunctional autophagy-DU145 cells, which have defective autophagy machinery due to the deficiency of a critical autophagy-related protein ATG5 (15) and 24-hour inhibition of autophagy by autophinib or SAR405.

Material and methods

Cell lines

Three human prostatic cell lines were used in this study. The human prostate carcinoma epithelial cell line 22Rv1is derived from a xenograft serially propagated in mice after castration. The cell line expresses prostate-specific antigen (PSA). Its growth is weakly stimulated by dihydroxy testosterone and lysates are immunoreactive with androgen receptor antibodies. The 22Rv1 line is PTEN-positive (16). The 22Rv1 cells have a heterozygous (p53$^{wt/mut}$) missense mutation (Q331R) in the tetramerization domain (amino acids 323–363) of p53 (17). PC-3 human epithelial cell line was established from a 4-grade prostatic adenocarcinoma, androgen-independent and unresponsive metastatic site in bone. PC-3 is PTEN-negative (16, 18). DU145 is a PTEN$^{+/-}$cell line with epithelial morphology that was isolated from the brain of a 69-year-old male with prostate cancer (16). DU145 and PC-3 cells harbor pairs of deleted or inactivated p53 alleles and display a complete loss of p53 function. DU145 cells express a truncated,

nonfunctional, retinoblastoma (Rb) protein (17) and have defective autophagy machinery due to the deficiency of a critical autophagy-related gene product, the ATG5 protein. This explains the loss of ATG12–ATG5 conjugates (15).

All three cell lines used in this study were purchased from HPA Culture Collections (Salisbury, UK). All cell lines were cultured in RPMI-1640 medium with 10 % FBS and supplemented with antibiotics (penicillin 100 U/ml and streptomycin 0.1 mg/ml). Cells were maintained at 37 °C in a humidified (60 %) incubator with 5 % CO_2 (Sanyo, Japan). The passages of cell lines ranged from 10 to 35. RPMI-1640 medium, fetal bovine serum (FBS) (mycoplasma-free), penicillin/streptomycin, and trypsin were purchased from Sigma Aldrich Co. (St. Louis, MO, USA). Phosphate-buffered saline PBS was purchased from Invitrogen Corp. (Carlsbad, CA, USA). Ethylenediaminetetraacetic acid (EDTA) and all other chemicals of ACS purity were purchased from Sigma Aldrich Co. (St. Louis, MO, USA). Concentrations for cisplatin treatments were derived from the MTT assay (IC_{25} values after 24h-treatment were 50 µmol/l for PC-3, 17.5 µmol/l for 22Rv1, and 12.5 µmol/l for DU145). MTT assay is based on the activity of NAD(P)H-dependent cellular oxidoreductase enzymes reducing the tetrazolium dye 3-(4,5-dimethylthiazol-2-yl)-2,5-diphenyltetrazolium bromide to insoluble formazan, which has a purple color. In experiments, IC_{25} concentrations of cisplatin were used.

Colony-forming assay

Cancer cells were seeded in 6-well plates and left to adhere overnight. Cells were seeded at 1,000 cells per well. Cisplatin treatment was added after 24 h and let to form colonies for 2 weeks. After cultivation, the colonies were fixed with cold methanol, visualized by trypan blue, and analyzed. For analysis, regions of interest were chosen by registering each image to the reference image (with the manually labelled area of interest). Next, the colonies were segmented by thresholding of the blue component of the image transformed into Lab color space, where a single fixed threshold was used. Finally, the fraction of areas covered by colonies was computed.

Live-cell metabolic assay Seahorse

The assay was performed according to the manufacturer's instructions. Briefly, cells were seeded at the density of $1x10^5$ cells per well in a Seahorse 24-well plate (Agilent Technologies, USA) and incubated for 24 h at 37 °C in the chosen treatment (IC_{25} of cisplatin, 1 mmol/l AA, autophagy inhibitor: 50nM autophinib or 10µM SAR405). A day before the analysis, Seahorse cartilage (Agilent Technologies, USA) was hydrated and incubated at 37 °C without CO_2. On the day of the experiment, the Seahorse XFp analyzer (Agilent Technologies, USA) was calibrated using hydrated cartilage. The culture medium was changed to Seahorse XF RPMI medium, pH 7.4 (Agilent Technologies, USA). After incubating cells for 1 h at 37 °C without CO_2, the Seahorse XF Real-Time ATP Rate Assay was performed by measuring the extracellular acidification rates (ECAR) as a proxy for glycolytic readouts and the oxygen consumption rates (OCR) as a proxy for oxidative phosphorylation readouts. The data were acquired
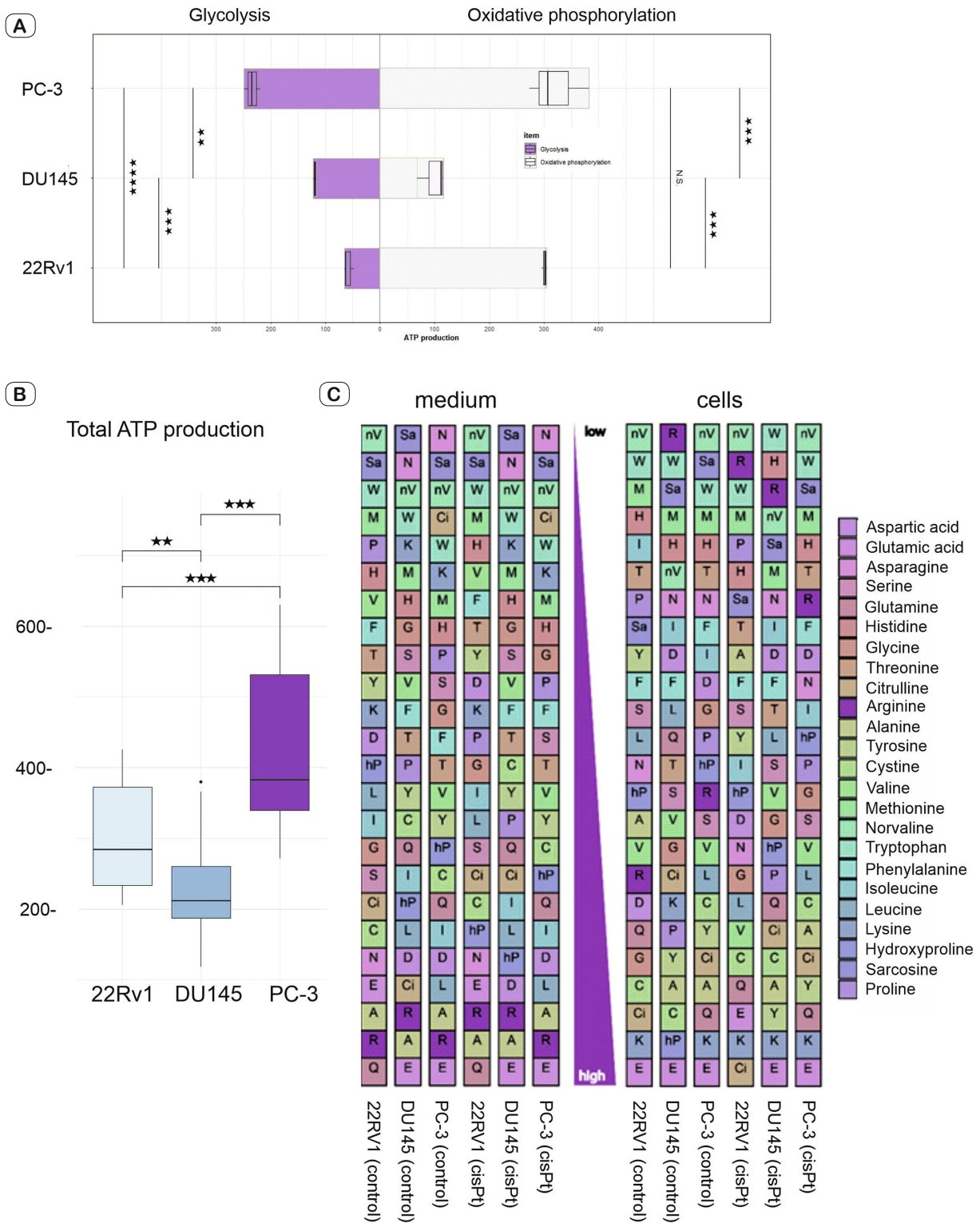
Fig.1. Metabolism of model cancer cells. A) ATP production via glycolysis and OXPHOS based on Seahorse parameters OCR and ECAR obtained from XF Real-Time ATP Rate Assay. p-values from group comparisons based on the t-test are shown. Asterisks represent statistical significance (* p < 0.05; ** p < 0.01; *** p < 0.001). B) Total ATP production in model cancer cells. P-values from group comparisons based on the t-test are shown. Asterisks represent statistical significance (* p < 0.05; ** p < 0.01; *** p < 0.001). C) Levels of amino acids in cells and medium before and after cisplatin treatment. Due to cisplatin treatment, a decrease in relative levels of arginine was observed in 22Rv1 and PC-3 cells. DU145 cells had a relative lack of arginine compared to 22Rv1 and PC-3 cells.

and analyzed using Wave Controller 2.4 software (Agilent Technologies, USA).

Quantitative phase imaging

The migration capacity of cancer cells was assessed using Tescan multimodal holographic microscope Q-PHASE which is based on the original concept of a coherence-controlled holographic microscope. Measurements were carried out under conditions optimized in our previous study (19). Briefly, cells were cultivated in flow chambers µ-Slide I Lauer Family (Ibidi, Germany). To obtain an image of a sufficient number of cells in one field of view, lens Nikon Plan 10/0.30 was chosen. Holograms were captured by a CCD camera (XIMEA, Slovakia). Complete image reconstruction and image processing were performed in Q-PHASE control software.

Amino acids profiling

Determination of amino acids was performed by high-performance liquid chromatography with fluorescence detection. An HP 1100 (Hewlett-Packard, Waldbronn, Germany) chromatographic system with a fluorescence detector (FLD) was used. A Zorbax Eclipse AAA chromatographic column (Agilent Technologies, California USA) with dimension 4.6×150 mm, and 3.5 µm particle size was used. The column effluent was monitored with a fluorescence detector at ex/em 340/450 nm and 266/305 nm respectively using the o-phtalaldehyde (OPA) for primary amino acids and 9-fluorenylmethyl chloroformate (FMOC) for secondary amino acids reagents for pre-column derivatization. The fluorescence wavelengths were switched at 14.52 min.

Mobile phase A, 40 mM Na 2 HPO 4 adjusted to pH 7,8 with 10 M NaOH solution; mobile phase B, ACN/MeOH/water (45:45:10 v/v/v); gradient, from 0 min 0 % B, 1.9 min 0 % B, 18.1 min 57 % B, 18.6 min 100 % B, 22.3 min 100 % B, 23.2 min 0 % B to 26 min; flow rate 2 mL/min; temperature of the column oven 40 °C was applied. The concentrations of individual amino acids were calculated based on the calculation of the linear regression equation from constructed calibration curves. Measurements were carried out under conditions optimized in (20).

Statistical analysis

The statistical analysis was performed using R 4.0.2 language (http://www.R-project.org/) with the following packages: ggplot2, tidyverse, corrplot, rstatix (21-24). Pearson correlation was computed to analyze the data in preparation for assessing the overall effects of treatments, ANOVA was used with simple t-tests or Tukey HSD as post hoc analysis. Unless noted otherwise $p < 0.05$ was considered significant.

Results

Prostate cancer cell lines differ in ATP production

To examine the predominant type of metabolism in our model cancer cells (22Rv1, PC-3, DU145), we used Seahorse XF Real-Time ATP Rate Assay Kit (Fig. 1A). This assay quantifies the rate of adenosine triphosphate (ATP) production from glycolysis and mitochondrial oxidative phosphorylation (OXPHOS) simultaneously using label-free technology in live cells. The PTEN-positive 22Rv1 cells derived from the primary tumor showed a high proportion of OXPHOS but ATP production from glycolysis was significantly lower compared to cells derived from metastases. The amount of glutamate and hydroxyproline in the culture medium of 22Rv1 cells positively correlated with total ATP production. The amounts of glutamine and tryptophan in the medium were negatively correlated with total ATP production.

The highest production of ATP was observable in PC-3 cells. The amounts of cystine and glycine in the culture medium were positively correlated with total ATP production in PC-3 cells. The amount of serine in the medium was negatively correlated with total ATP production.

On the other hand, DU145 cells had the lowest total ATP production (Fig. 1B), and they also were the most sensitive to cisplatin (IC_{25} value of cisplatin was 12.5 µmol/l for DU145, 50 µmol/l for PC-3, and 17.5 µmol/l for 22Rv1). In DU145, the amounts of serine, alanine, and lysine in the medium correlated negatively with total ATP production. DU145 cells had also a relative lack of arginine compared to 22Rv1 and PC-3 cells (Fig. 1C). Due to cisplatin treatment, a decrease in the levels of arginine (relative to other amino acids) was observed in 22Rv1 and PC-3 cells, suggesting that cisplatin interferes with arginine metabolism (Fig.1C). As the depletion of arginine induces autophagy as a cytoprotective response and DU145 cells are autophagy-incompetent, it may contribute to their sensitivity to cisplatin. Therefore, we set out to determine whether inhibition of autophagy with autophinib or SAR405 would lead to increased metabolic sensitivity to cisplatin in the PC-3 and 22Rv1 lines known to have functional autophagy machinery (25).

The short-term autophagy inhibition has no effect on metabolic sensitivity to cisplatin

After cisplatin treatment, ATP production by OXPHOS was significantly decreased in 22Rv1 and PC-3 cells. On the other hand, ATP production by glycolysis was not significantly affected in 22Rv1 cells (Fig. 2A). The addition of 1 mmol/l methionine to the culture medium attenuated OXPHOS in 22Rv1 cells (Fig. 2B). Autophagy inhibition (24-hour exposure to inhibitors) did not change the effect of cisplatin in PC-3 or 22Rv1 cells. On the contrary, SAR405 treatment slightly enhanced the ATP production via OXPHOS in DU145 cells during cisplatin exposure (Fig. 2A).

To assess the motility of cancer cells, a scratch test was performed. As expected, 22Rv1 cells (derived from the primary tumor) hardly moved and their motility was negligible compared to metastasis-derived cells (Fig. 3A). Cisplatin significantly enhanced the free area showing a lower motility of cancer cells (Fig. 3B). The speed of motion of metastatic cells (PC-3) was also significantly decreased by cisplatin (Fig. 3C). Cisplatin also significantly decreased the number of colonies, but in PTEN-defective metastatic cells (PC-3, DU145), this effect was more prominent (Fig. 3D). The concentration of 1 mmol/l lactate supported the growth of metastatic cell colonies but decreased the growth of 22RV1 colonies (Fig. 3E).
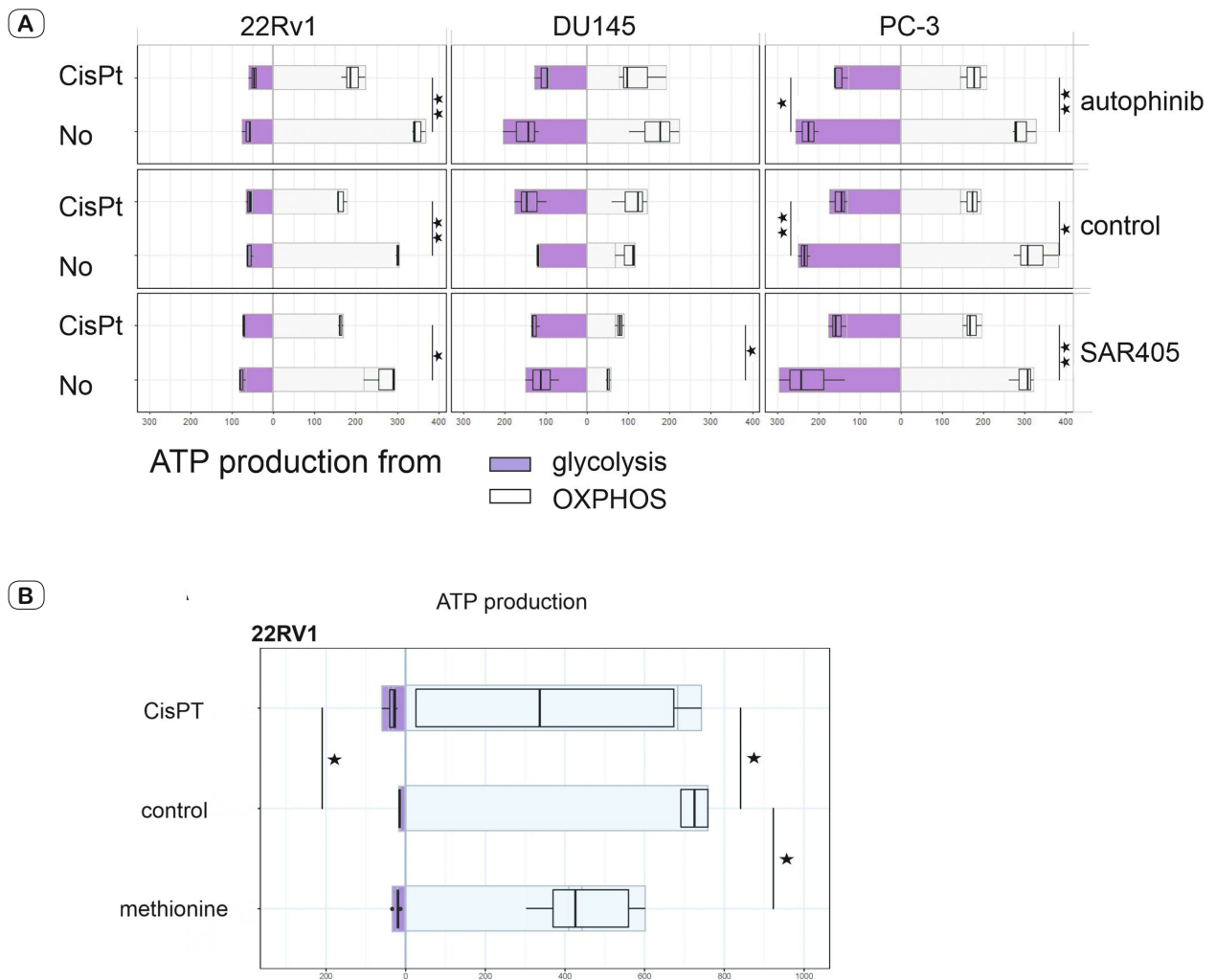
Fig. 2. Metabolism of model cancer cells. A) ATP production via glycolysis and OXPHOS based on Seahorse parameters OCR and ECAR obtained from XF Real-Time ATP Rate Assay before and after cisplatin/autophagy inhibitor treatment. p-values from group comparisons based on the t-test are shown. Asterisks represent statistical significance (* p < 0.05; ** p < 0.01; *** p < 0.001). B) Total ATP production in 22RV1 cells before and after cisplatin/methionine treatment. p-values from group comparisons based on the t-test are shown. Asterisks represent statistical significance (* p < 0.05; ** p < 0.01; *** p < 0.001).

Discussion

Most cancers become less efficient in energy production as they undergo malignant transformation accompanied by the Warburg effect. On the other hand, prostate cancer cells become more energy-efficient as their malignant transformation includes the switch from citrate-secreting cells to citrate-oxidizing cells, allowing an increased flow through the TCA cycle. This metabolic transformation is an early event in prostate tumorigenesis (26). Changes in glucose metabolism, amino acid pool, and other metabolic pathways can deeply affect the cisplatin resistance of cancer cells (27). Here, we assessed the metabolic and amino acid profiles of model cancer cell lines depicting prostate cancer progression. The 22Rv1 cell line is PTEN-positive (16) with a heterozygous (p53wt/ mut) missense mutation in p53 (17) used by us as a model of the

primary prostatic tumors. PC-3 acts as a PTEN-negative androgen unresponsive metastatic bone tumor with inactivated p53 (16, 18). DU145 cells were used as a PTEN+/−, p53-negative, Rb-negative cell line model of brain metastases derived from prostate tumor (16, 17). DU145 cells have a defect in autophagy machinery due to the loss of ATG12–ATG5 conjugates (15). DU145 cells had the lowest total ATP production, and they were the most sensitive to cisplatin (IC25 value was 12.5 µmol/l) and have also a relative lack of arginine compared to 22Rv1 and PC-3 cells. The lack of arginine in DU145 cells can be caused by the loss of functional ATG12–ATG5 conjugates. The emergence of functional ATG12– ATG5 conjugates is regulated by ATG7 (28). Consequently, the loss of functional ATG12–ATG5 conjugates can upregulate the expression of Arginase I (ARG1) which is a cytosolic enzyme that catalyzes the hydrolysis of L-arginine (29). Due to cisplatin
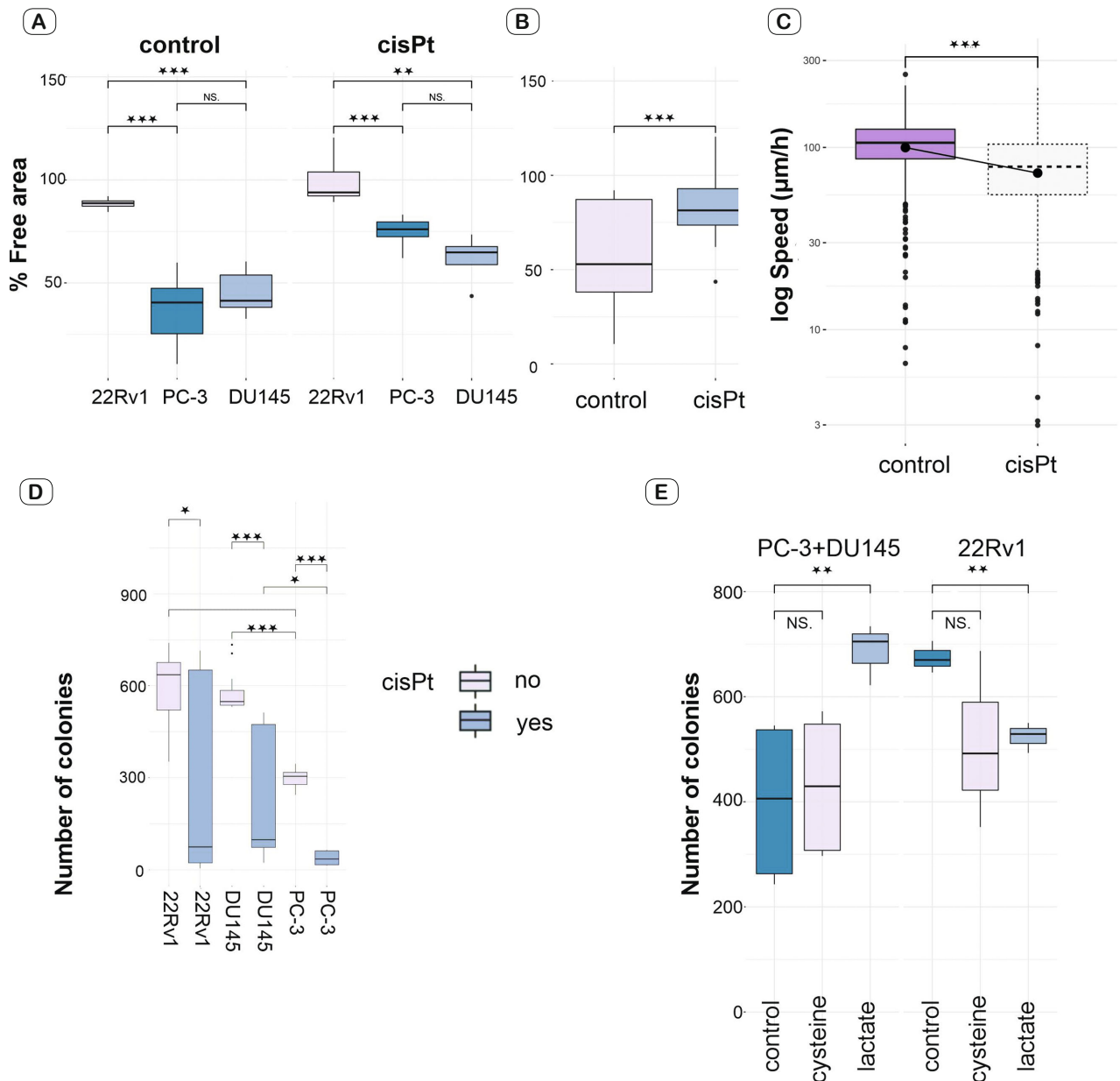
Fig. 3. Motility and colony-forming potential. A) Scratch test in nontreated cells and after cisplatin treatment. B) Scratch test; cisplatin significantly enhanced free area showing lower motility of cancer cells. C) Cell speed calculated from QPI (Quantitative Phase Imaging). D) Colony-forming assay; effect of cisplatin. E) Colony-forming assay; effect of cysteine and lactate. p-values from group comparisons based on the t-test are shown. Asterisks represent statistical significance (* p < 0.05; ** p < 0.01; *** p < 0.001).

treatment, a decrease in relative levels of arginine was observed in 22Rv1 and PC-3 cells. It was reported that cisplatin suppresses *de novo* biosynthesis of arginine by argininosuccinate synthetase 1 (ASS1) (30). Consequently, cisplatin-treated cells can develop a dependency on arginine. DU145 cells are disadvantaged in arginine synthesis from the start (due to the autophagy defect), which may contribute to their higher sensitivity to cisplatin. Moreover, the depletion of arginine induces autophagy as a cytoprotective response while DU145 cells are autophagy-incompetent, which may further contribute to their sensitivity to cisplatin (31). Nev-

ertheless, short-term autophagy inhibition (24-hour exposure to VPS34 inhibitors autophinib or SAR405) did not change the metabolic effect of cisplatin in PC-3 or 22Rv1 cells. Surprisingly, SAR405 treatment slightly enhanced ATP production via OXPHOS in DU145 cells during cisplatin exposure. This effect is probably associated with the role of VPS34 in PI3P production and oxidative stress management (32, 33).

After cisplatin treatment, the ATP production via OXPHOS was significantly decreased in 22Rv1 and PC-3 cells. On the other hand, the ATP production by glycolysis was not significantly af-

fected in 22Rv1 cells. The amount of glutamate and hydroxyproline in the culture medium of 22Rv1 cells positively correlated with total ATP production. On the contrary, the amounts of glutamine and tryptophan in the medium were negatively correlated with total ATP production. The high levels of glutamine in the medium may point to the low activity of glutaminase and attenuation of glutaminolysis. On the other hand, high levels of glutamate can be caused by the activation of glutaminolysis, which is a hallmark of cancer metabolism. The first step in the process of glutaminolysis involves a conversion of glutamine into glutamate via glutaminase (GLS/GLS2) (34). Surprisingly, the addition of 1 mmol/l methionine to the culture medium attenuated the OXPHOS pathway in 22Rv1 cells. Methionine is a direct target of reactive oxygen species (ROS), as its sulfur can be oxidized, transforming methionine into methionine sulfoxide (MetO). Due to the repair of MetO through methionine sulfoxide reductases, methionine can act as a scavenger and protect cells from oxidative stress. Nevertheless, accumulated MetO may act as an inhibitor of Met metabolism and can contribute to the exacerbation of oxidative stress (35).

After cisplatin treatment, total ATP production, cell speed, and the number of colonies were significantly decreased in metastatic cancer cells. Moreover, PTEN-defective PC-3 cells seemed to be more prone to the effects of cisplatin on colony-forming ability. Depletion of PTEN impairs mitochondrial structure and respiratory chain function (10) and therefore it is crucial for PTEN-negative cells to keep high mitochondria fitness through proper defense against reactive oxygen species (ROS). Recent evidence in humans and mice supports the notion that mitochondrial metabolism is necessary for tumor growth (12). The amount of cysteine and glycine in the culture medium positively correlated with total ATP production in PC-3. Cysteine and glycine are glutathione precursors and therefore, they can lower the levels of oxidative stress and oxidant damage (36).

The addition of 1 mmol/l lactate supported the growth of metastatic cell colonies but decreased the growth of 22RV1 colonies. Although long considered to be a metabolic waste product, lactate plays a critical role in carcinogenic signaling, fueling the proliferation of cancer cells, and supporting metastasis and tumor resistance (37). Nevertheless, lactate can promote a HIF-1α-mediated metabolic shift from OXPHOS to glycolysis, which can disrupt the ability of citrate-oxidizing prostate cancer cells to grow (26, 38).

In conclusion, it was shown that short-term autophagy inhibition (24h) by autophinib or SAR405 does not alter the effect of cisplatin on ATP production in prostate cancer cells. On the other hand, persistent defects of the autophagy machinery can affect the metabolic sensitivity of prostate cancer cells due to interfering with arginine metabolism. It was also shown that the amino acids contained in the culture medium had a significant impact on the overall effect of cisplatin.

References

1. de Vries G, Rosas-Plaza X, van Vugt MATM, Gietema JA, de Jong S. Testicular cancer: Determinants of cisplatin sensitivity and novel therapeutic opportunities. Cancer Treatment Rev 2020; 88: 102054.

2. Peltanova B, Liskova M, Gumulec J, Raudenska M, Polanska HH, Vaculovic T et al. Sensitivity to Cisplatin in Head and Neck Cancer Cells Is Significantly Affected by Patient-Derived Cancer-Associated Fibroblasts. Int J Mol Sci 2021; 22 (4).

3. Schmid S, Omlin A, Higano C, Sweeney C, Martinez Chanza N, Mehra N et al. Activity of Platinum-Based Chemotherapy in Patients With Advanced Prostate Cancer With and Without DNA Repair Gene Aberrations. JAMA Network Open 2020; 3 (10): e2021692-e.

4. Amsberg GV, Zilles M, Gild P, Alsdorf W, Boeckelmann L, Langebrake C et al. Salvage chemotherapy with cisplatin, ifosfamide, and paclitaxel in metastatic castration-resistant prostate cancer. J Clin Oncol 2021; 39 (Suppl 6): 123.

5. Gumulec J, Balvan J, Svobodová M, Raudenska M, Dvorakova V, Knopfova L et al. Cisplatin-resistant prostate cancer model: Differences in antioxidant system, apoptosis and cell cycle. Internat J Oncol 2014; 44: 923–933.

6. Raudenska M, Kratochvilova M, Vicar T, Gumulec J, Balvan J, Polanska H et al. Cisplatin enhances cell stiffness and decreases invasiveness rate in prostate cancer cells by actin accumulation. Sci Reports 2019; 9 (1): 1660.

7. Raudenska M, Balvan J, Fojtu M, Gumulec J, Masarik M. Unexpected therapeutic effects of cisplatin. Metallomics 2019; 11 (7): 1182–1199.

8. Kartalou M, Essigmann JM. Mechanisms of resistance to cisplatin. Mutat Res 2001; 478 (1–2): 23–43.

9. Kleih M, Böpple K, Dong M, Gaißler A, Heine S, Olayioye MA et al. Direct impact of cisplatin on mitochondria induces ROS production that dictates cell fate of ovarian cancer cells. Cell Death Dis 2019; 10 (11): 851.

10. Liang H, He S, Yang J, Jia X, Wang P, Chen X et al. PTENα, a PTEN Isoform Translated through Alternative Initiation, Regulates Mitochondrial Function and Energy Metabolism. Cell Metab 2014; 19 (5): 836–848.

11. Garrido N, Pérez-Martos A, Faro M, Lou-Bonafonte JM, Fernández-Silva P, López-Pérez MJ et al. Cisplatin-mediated impairment of mitochondrial DNA metabolism inversely correlates with glutathione levels. Biochem J 2008; 414 (1): 93–102.

12. Bajzikova M, Kovarova J, Coelho AR, Boukalova S, Oh S, Rohlenova K et al. Reactivation of Dihydroorotate Dehydrogenase-Driven Pyrimidine Biosynthesis Restores Tumor Growth of Respiration-Deficient Cancer Cells. Cell Metab 2019; 29 (2): 399–416 e10.

13. Vasan K, Werner M, Chandel NS. Mitochondrial Metabolism as a Target for Cancer Therapy. Cell Metab 2020; 32 (3): 341–352.

14. Gunda V, Pathania AS, Chava S, Prathipati P, Chaturvedi NK, Coulter DW et al. Amino Acids Regulate Cisplatin Insensitivity in Neuroblastoma. Cancers (Basel) 2020; 12 (9).

15. Ouyang DY, Xu LH, He XH, Zhang YT, Zeng LH, Cai JY et al. Autophagy is differentially induced in prostate cancer LNCaP, DU145 and PC-3 cells via distinct splicing profiles of ATG5. Autophagy 2013; 9 (1): 20–32.

16. Fraser M, Zhao H, Luoto KR, Lundin C, Coackley C, Chan N et al. PTEN deletion in prostate cancer cells does not associate with loss of RAD51 function: implications for radiotherapy and chemotherapy. Clin Cancer Res 2012; 18 (4): 1015–1027.

17. Lehmann BD, McCubrey JA, Jefferson HS, Paine MS, Chappell WH, Terrian DM. A Dominant Role for p53-Dependent Cellular Senescence in Radiosensitization of Human Prostate Cancer Cells. Cell Cycle 2007; 6 (5): 595–605.

18. Gumulec J, Balvan J, Sztalmachova M, Raudenska M, Dvorakova V, Knopfova L et al. Cisplatin-resistant prostate cancer model: Differences in antioxidant system, apoptosis and cell cycle. Int J Oncol 2014; 44 (3): 923–933.

19. Vicar T, Raudenska M, Gumulec J, Balvan J. The Quantitative-Phase Dynamics of Apoptosis and Lytic Cell Death. Sci Reports 2020; 10 (1): 1566.

20. Vsiansky V, Svobodova M, Gumulec J, Cernei N, Sterbova D, Zitka O et al. Prognostic Significance of Serum Free Amino Acids in Head and Neck Cancers. Cells 2019; 8 (5).

21. Wickham H. ggplot2: Elegant Graphics for Data Analysis: Springer Publishing Company, Incorporated; 2016.

22. Wickham H, Averick M, Bryan J, Chang W, McGowan L, François R et al. Welcome to the Tidyverse. J Open Source Software 2019; 4: 1686.

23. Wei T, Simko V. R package "corrplot": Visualization of a Correlation Matrix. 0.92 ed2021.

24. Kassambara A. Pipe-Friendly Framework for Basic Statistical Tests [R package rstatix version 0.7.0] 2021.

25. Hahm ER, Singh SV. Cytoprotective autophagy induction by withaferin A in prostate cancer cells involves GABARAPL1. Mol Carcinog 2020; 59 (10): 1105–1115.

26. Costello LC, Franklin RB. Citrate metabolism of normal and malignant prostate epithelial cells. Urology 1997; 50 (1): 3–12.

27. Wang L, Zhao X, Fu J, Xu W, Yuan J. The Role of Tumour Metabolism in Cisplatin Resistance. Front Mol Biosci 2021; 8: 691795.

28. Collier JJ, Suomi F, Oláhová M, McWilliams TG, Taylor RW. Emerging roles of ATG7 in human health and disease. EMBO Molecular Medicine 2021; 13 (12): e14824.

29. Poillet-Perez L, Xie X, Zhan L, Yang Y, Sharp DW, Hu ZS et al. Autophagy maintains tumour growth through circulating arginine. Nature 2018; 563 (7732): 569–573.

30. Long Y, Tsai WB, Chang JT, Estecio M, Wangpaichitr M, Savaraj N et al. Cisplatin-induced synthetic lethality to arginine-starvation therapy by transcriptional suppression of ASS1 is regulated by DEC1, HIF-1α, and c-Myc transcription network and is independent of ASS1 promoter DNA methylation. Oncotarget 2016; 7 (50): 82658–82670.

31. García-Navas R, Munder M, Mollinedo F. Depletion of L-arginine induces autophagy as a cytoprotective response to endoplasmic reticulum stress in human T lymphocytes. Autophagy 2012; 8 (11): 1557–1576.

32. Kaminska J, Rzepnikowska W, Polak A, Flis K, Soczewka P, Bala K et al. Phosphatidylinositol-3-phosphate regulates response of cells to proteotoxic stress. Internat J Biochem Cell Biol 2016; 79: 494–504.

33. Jiang X, Bao Y, Liu H, Kou X, Zhang Z, Sun F et al. VPS34 stimulation of p62 phosphorylation for cancer progression. Oncogene 2017; 36 (50): 6850–6862.

34. Yang L, Venneti S, Nagrath D. Glutaminolysis: A Hallmark of Cancer Metabolism. Ann Rev Biomed Engineering 2017; 19 (1): 163–194.

35. Lee BC, Gladyshev VN. The biological significance of methionine sulfoxide stereochemistry. Free Radic Biol Med 2011; 50 (2): 221–227.

36. Sekhar RV, Patel SG, Guthikonda AP, Reid M, Balasubramanyam A, Taffet GE et al. Deficient synthesis of glutathione underlies oxidative stress in aging and can be corrected by dietary cysteine and glycine supplementation. Am J Clin Nutr 2011; 94 (3): 847–853.

37. Pérez-Tomás R, Pérez-Guillén I. Lactate in the Tumor Microenvironment: An Essential Molecule in Cancer Progression and Treatment. Cancers (Basel) 2020; 12 (11).

38. Kozlov AM, Lone A, Betts DH, Cumming RC. Lactate preconditioning promotes a HIF-1α-mediated metabolic shift from OXPHOS to glycolysis in normal human diploid fibroblasts. Sci Rep 2020; 10 (1): 8388.